XTE J1814-338 as a Strange Star Admixed with Bosonic Dark Matter

Shuhua Yang(杨书华)[1*] and Fridolin Weber[2,3*]

[1]*Institute of Astrophysics, Central China Normal University, Wuhan 430079, China*
[2]*Department of Physics, San Diego State University, San Diego, CA 92182, USA*
[3]*Department of Physics, University of California at San Diego, La Jolla, CA 92093, USA*

(Received 28 October 2025; accepted manuscript online 23 December 2025)

We show that the compact star XTE J1814-338 can be explained as a strange star admixed with self-interacting bosonic dark matter (BDM), provided the dark matter fraction exceeds approximately 70%. This interpretation leads to a robust constraint on the BDM particle mass: $m_\chi \lesssim 307(\lambda/\pi)^{1/4}$ MeV (λ is the dimensionless coupling constant of the BDM). The result is independent of formation scenario and microphysical details and is falsifiable by future NICER and LIGO/Virgo observations.

DOI: 10.1088/0256-307X/43/2/021102 CSTR: 32039.14.0256-307X.43.2.021102

1. Introduction. According to strange quark matter (SQM) hypothesis,[1–4] SQM consists of roughly equal numbers of up (u), down (d), and strange (s) quarks, along with a small admixture of electrons, which may be more stable than ordinary nuclear matter. As a consequence, compact stars could exist as strange stars (SSs)[5–8] rather than neutron stars (NSs). Interestingly, it is found recently that SSs could well explain the repeating fast radio bursts,[9] and also the anomalous X-ray pulsars and soft gamma-ray repeaters.[10]

Compact stars, NSs and SSs, might contain a dark matter (DM) core or a DM halo made of non-annihilating self-interacting DM.[11,12] Thus, it is expected that the observations of compact stars could help us to unveil the nature of DM.

Recently, the mass and radius of the Type I X-ray burster and accretion-powered millisecond pulsar XTE J1814-338 were inferred to be $M = 1.21 \pm 0.05 M_\odot$ and $R = 7.0 \pm 0.4$ km (68.3% credibility interval), using the pulse-profile modeling technique.[13] To explain such unusually low mass and radius of XTE J1814-338, a theoretical model beyond conventional NSs composed of standard nuclear matter is needed. Several studies have tried to explain the observations of XTE J1814-338 as hybrid stars,[14–16] while others speculate that XTE J1814-338 might be a DM admixed NS[17,18] or a DM admixed SS.[19,20]

In this Letter, we will explain the observations of XTE J1814-338 assuming it is an SS admixed with bosonic dark matter (BDM).[21,22] Although the SSs admixed with BDM have been studied recently by Liu *et al.*,[23] this work will extend their study to higher values of the fraction of BDM in SSs, which is necessary for us to explain the mass and radius observations of XTE J1814-338. Moreover, we will constrain the mass of the BDM using the observations of XTE J1814-338. This work employs a different SQM model than Ref. [23].

Compared with neutron or hybrid star models, SSs provide a natural explanation for compact objects with exceptionally small radii. The self-bound nature of SQM permits more compact configurations at relatively low gravitational mass. In this regard, XTE J1814-338 is particularly interesting, as its inferred radius of $R = 7.0 \pm 0.4$ km is difficult to reconcile with conventional hadronic equations of state, but fits well within the predictions of BDM-admixed SSs. This motivates our investigation within the SS framework, rather than adopting a nuclear or hybrid star model.

2. Equation of State of SQM and BDM. For the equation of state (EOS) of SQM, we employ the modified MIT bag model, where u and d quarks are considered to be massless, while the s quark has a finite[4,5,7,24] mass ($m_{\rm s} = 93$ MeV[25]). In this model, first-order perturbative corrections to the strong interaction coupling constant $\alpha_{\rm S}$ are included to account for interactions among quarks. Given the thermodynamic potentials for u, d, s quarks, and electrons (Ω_i, which can be found in Refs. [5,26,27]), the number density of each species is

$$n_i = -\frac{\partial \Omega_i}{\partial \mu_i}, \tag{1}$$

where μ_i ($i = u, d, s, e$) are the chemical potentials. For SQM, the chemical equilibrium is maintained by the weak-interaction processes and one has

$$\mu_{\rm d} = \mu_{\rm s}, \quad \mu_{\rm s} = \mu_{\rm u} + \mu_{\rm e}. \tag{2}$$

The charge neutrality equation is given by

$$\frac{2}{3} n_{\rm u} - \frac{1}{3} n_{\rm d} - \frac{1}{3} n_{\rm s} - n_{\rm e} = 0. \tag{3}$$

The energy density and pressure of SQM are then given by

$$\epsilon_{\rm Q} = \sum_{i={\rm u,d,s,e}} (\Omega_i + \mu_i n_i) + B, \tag{4}$$

$$p_{\rm Q} = -\sum_{i={\rm u,d,s,e}} \Omega_i - B, \tag{5}$$

*Corresponding authors. Email: ysh@ccnu.edu.cn; fweber@ucsd.edu
© 2026 Chinese Physical Society and IOP Publishing Ltd. All rights, including for text and data mining, AI training, and similar technologies, are reserved.

where B is the bag constant. The EOS of BDM with a repulsive self-interaction is given by [22,28,29]

$$p_{\rm D} = \frac{m_\chi^4}{9\lambda}\left(\sqrt{1+\frac{3\lambda}{m_\chi^4}\epsilon_{\rm D}}-1\right)^2, \tag{6}$$

where $\epsilon_{\rm D}$ and $p_{\rm D}$ are the energy density and pressure of BDM, respectively; m_χ is the BDM particle mass; λ is the dimensionless coupling constant. Derivation of Eq. (6) can be found in Ref. [28]. Defining $\epsilon_0 \equiv m_\chi^4/(4\lambda)$, one has [23,30]

$$p_{\rm D} = \frac{4\epsilon_0}{9}\left(\sqrt{1+\frac{3}{4\epsilon_0}\epsilon_{\rm D}}-1\right)^2. \tag{7}$$

Apparently, instead of two parameters (m_χ and λ), this EOS only depends on one parameter ϵ_0.

For the quartic BDM model used here (the BDM particles are described by a complex scalar field with the self-interaction potential $V(\phi) = \lambda|\phi|^4/4$),[22,28] the self-interaction cross section per unit mass is $\sigma/m_\chi = \lambda^2/(16\pi m_\chi^3)$ in natural units.[23,30,31] For the parameter range relevant to XTE J1814-338 ($\lambda = \pi$, $m_\chi \sim 200$–$350\,$MeV), this yields $\sigma/m_\chi \sim 10^{-3}\,{\rm cm}^2\cdot{\rm g}^{-1}$, which is orders of magnitude below astrophysical limits ($\sigma/m_\chi \lesssim 0.1$–$1\,{\rm cm}^2\cdot{\rm g}^{-1}$).[32–34]

In this work, we focus on cold catalyzed matter and adopt zero-temperature EOS for both the SQM and the BDM components. This is a valid approximation for old, thermally relaxed compact stars such as XTE J1814-338. For proto-SSs or post-merger remnants, thermal corrections may become relevant[35–38] and will be addressed in future work.

3. Results. We now derive constraints on the BDM particle mass from the observed mass and radius of XTE J1814-338. For the given EOS of SQM and BDM, we investigate the structure of SSs admixed with BDM using the two-fluid formalism,[19,39–44] which means that we assume the SQM and BDM components interact only through gravity, with no direct interactions between them. In our calculation, the mass fraction of BDM is defined as $f_{\rm D} \equiv M_{\rm D}/M$, where M is the total mass of the star and $M_{\rm D}$ is the mass of the BDM component.

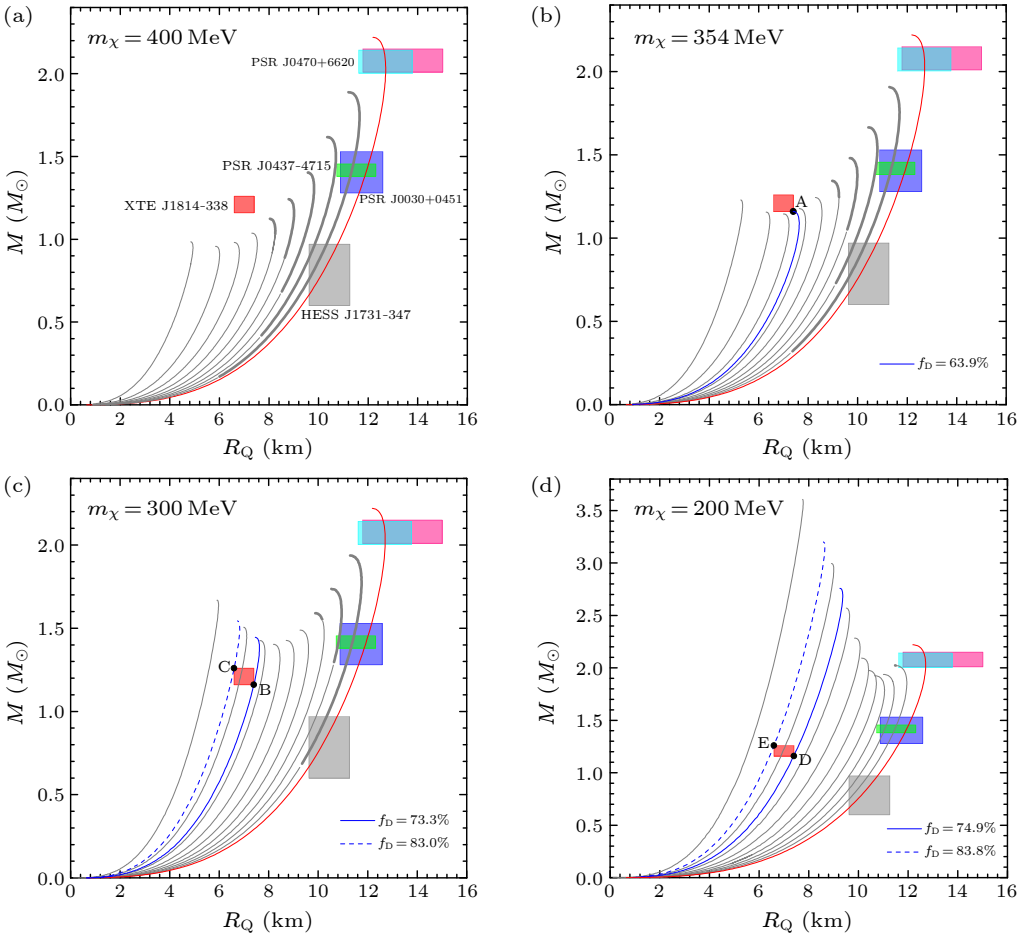

Fig. 1. Mass-radius relations for BDM-admixed SSs, with $R_{\rm Q}$ denoting the radius of the SQM component. All models are computed using $\alpha_{\rm S} = 0.6$, $B^{1/4} = 135\,$MeV, and $\lambda = \pi$. (a)–(d) The boson masses $m_\chi = 400$, 354, 300, and 200 MeV, respectively. The red curve in each panel shows the pure SS case ($f_{\rm D} = 0\%$), while gray curves represent varying BDM mass fractions from $f_{\rm D} = 10\%$ to 90% in steps of 10%. Thick segments correspond to configurations with a DM core; thin segments indicate DM halos (a "DM core" refers to configurations in which the DM radius does not exceed the SQM radius, while a "DM halo" denotes configurations with an extended DM distribution surrounding the SQM core). Black dots mark the benchmark stellar models listed in Table 1. Colored bands show observational constraints from: XTE J1814-338 (red),[13] PSR J0740+6620 (pink/cyan),[45–48] PSR J0030+0451 (blue),[49] PSR J0437-4715 (green),[50] and HESS J1731-347 (gray).[51]

Table 1. Parameters of five BDM-admixed SS models that satisfy the mass and radius constraints of XTE J1814-338. $R_{\rm D}$ is the total radius of the star (i.e., the outer radius of the BDM halo), $M(R_{\rm Q})$ is the enclosed gravitational mass at the surface of the SQM core, and $M_{\rm c}$ is the BDM mass outside $R_{\rm Q}$.

Model	m_χ (MeV)	$f_{\rm D}$ (%)	M ($M_\odot$)	$R_{\rm Q}$ (km)	$M_{\rm D}$ ($M_\odot$)	$R_{\rm D}$ (km)	$M(R_{\rm Q})$ ($M_\odot$)	$M_{\rm c}$ ($M_\odot$)	$M_{\rm c}/M_{\rm D}$
A	354	63.9	1.16	7.40	0.741	9.19	1.096	0.064	0.086
B	300	73.3	1.16	7.40	0.850	18.03	0.566	0.594	0.699
C	300	83.0	1.26	6.60	1.046	19.81	0.403	0.857	0.820
D	200	74.9	1.16	7.40	0.869	48.18	0.320	0.840	0.967
E	200	83.8	1.26	6.60	1.056	52.81	0.222	1.038	0.983

As shown in Fig. 1(a), the mass and radius of XTE J1814-338 cannot be satisfied when $m_\chi = 400\,\text{MeV}$. However, the curves move upward as the value of m_χ becomes smaller, and the observations of XTE J1814-338 can be marginally satisfied for the case of $m_\chi = 354\,\text{MeV}$, supposing the BDM mass fraction of the star is $f_{\rm D} = 63.9\%$, see Fig. 1(b). If $m_\chi < 354\,\text{MeV}$, the observations of XTE J1814-338 could be well satisfied for certain ranges of the value of $f_{\rm D}$. For example, for the case of $m_\chi = 300\,\text{MeV}$, the BDM-admixed SSs with $f_{\rm D} = 73.3\%$–83.0% can explain the observations of XTE J1814-338 [Fig. 1(c)]. For another example, for the case of $m_\chi = 200\,\text{MeV}$, the BDM-admixed SSs with $f_{\rm D} = 74.9\%$–83.8% can explain the observations of XTE J1814-338 [Fig. 1(d)]. Note that to fulfill the observations of XTE J1814-338, the BDM mass fraction should be as high as $f_{\rm D} \sim 70\%$. In contrast, low values of $f_{\rm D}$ (less than ∼30%, even pure SS with $f_{\rm D} = 0$) could satisfy all the other observations shown in Fig. 1. This distinguishes XTE J1814-338 as a uniquely high-$f_{\rm D}$ object among observed compact stars, whereas others are consistent with low-$f_{\rm D}$ or pure SS configurations.

The parameters of the five stellar models marked by black dots in Figs. 1(b)–1(d) are shown in Table 1. We find that stellar model "A" has a compact DM halo, and the other four stellar models ("B","C","D", and "E") have an intermediate DM halo,[52] where a "DM halo" denotes configurations with an extended DM distribution surrounding the SQM core. Different from Ref. [52] with a small DM fraction ($f_{\rm D} = 5\%$), $f_{\rm D}$ is large for all the stellar models in Table 1. As a result, one cannot use the value of $M_{\rm c}/M_{\rm D}$ ($M_{\rm c}$ is the BDM mass located outside $R_{\rm Q}$, where $R_{\rm Q}$ denotes the radius of the SQM component, i.e., the visible surface) alone to distinguish the type of halos (compact, intermediate, or diffuse). In Ref. [52], the authors demonstrated that for the scenario of the diffuse halos, the mass measurement of XTE J1814-338 (which is determined through X-ray pulse-profile modeling[13]) corresponds to $M(R_{\rm Q})$ (the enclosed gravitational mass at $R_{\rm Q}$), while for the scenarios of the compact halos and the intermediate halos, the mass measurement of XTE J1814-338 will be very close to the total mass of the star (M). Therefore, it is more reasonable to choose M as the longitudinal axis in Fig. 1 rather than $M(R_{\rm Q})$. As for the radius, since photons are emitted from the surface of the SQM, the visible radius inferred from X-ray pulse-profile modeling corresponds to $R_{\rm Q}$, the radius of the baryonic component. We therefore treat $R_{\rm Q}$ as the observable radius throughout this work, in contrast to the total gravitational radius $R_{\rm D}$ of the full DM halo.

Our work leads to the conclusion that for $\alpha_{\rm S} = 0.6$, $B^{1/4} = 135\,\text{MeV}$, and $\lambda = \pi$, the observations of XTE J1814-338 constrain the boson mass of the BDM to $m_\chi \leq 354\,\text{MeV}$. Since $\epsilon_0 = m_\chi^4/(4\lambda)$ is the only parameter which the EOS of BDM depends on, the constraint to m_χ turns out to be $m_\chi \leq 354(\lambda/\pi)^{1/4}\,\text{MeV}$. This constraint could be reframed in terms of the compactness $\mathcal{C}_{\rm obs} = M/R_{\rm Q}$ inferred from observation. Specifically, XTE J1814-338 exhibits a compactness of $\mathcal{C}_{\rm obs} \approx 1.21\,M_\odot/7.0\,\text{km} \approx 0.173\,M_\odot/\text{km}$. We analyze the models in Table 1 and interpolate their corresponding compactness values as a function of the BDM EOS parameter ϵ_0. By extrapolating this relation, one finds that only models with $\epsilon_0 \lesssim 7.1 \times 10^8\,\text{MeV}^4$ can satisfy the compactness constraint. This yields a general upper bound,

$$m_\chi \lesssim 307\left(\frac{\lambda}{\pi}\right)^{1/4}\text{MeV}. \tag{8}$$

While this constraint is derived from XTE J1814-338, it is phrased in terms of compactness and applies to any compact object with similar mass–radius ratios, regardless of composition or formation history. Although the bound still depends on the existence of an extremely compact star, it does not rely on detailed assumptions about internal structure or DM distribution. Rather, it reflects a minimal requirement that any BDM+SS configuration must satisfy to reproduce such compactness.

We verify that these BDM-admixed SS configurations lie on the dynamically stable branch of the two-fluid sequence, well below the turning point at which $\mathrm{d}M/\mathrm{d}\rho_{\rm c}$ changes sign.*

4. Outlook. To place our results in the broader landscape of DM admixed compact star models, we compare the viability of SSs mixed with BDM, as presented in this work, against several existing frameworks, including NSs and SSs with similar dark sector interactions. Table 2 summarizes the extent to which each model can explain the mass and radius constraints of well-observed compact objects, such as XTE J1814-338, PSR J0740+6620, PSR J0030+0451, PSR J0437-4715, and HESS J1731-347.

*In multifluid stars, the onset of instability is associated with the turning point of the gravitational mass along the equilibrium sequence (e.g., Ref. [53]). For the one-parameter sequences shown in Fig. 1, this turning point occurs at the maximum mass, so all models lying on the $\mathrm{d}M/\mathrm{d}\rho_{\rm c} > 0$ side of this maximum belong to the stable branch.

Table 2. Comparison of compact star observations with different BDM-admixed models. "Viable" means the model satisfies mass and radius constraints under the authors' assumptions. For Karkevandi *et al.*,[28] this requires $f_{\rm D} \lesssim 5\%$ due to tidal deformability constraints. For Liu *et al.*,[30] high-$f_{\rm D}$ NSs are disfavored for $m_\chi \gtrsim 200\,{\rm MeV}$.

Object	Karkevandi *et al.*[28] (NS+BDM)	Liu *et al.*[30] (NS+BDM)	Liu *et al.*[23] (SS+BDM)	This work (SS+BDM)
XTE J1814-338	Not viable ($f_{\rm D} \lesssim 5\%$)	Viable ($f_{\rm D} \gtrsim 5\%$ plausible)	–	Viable ($m_\chi \leq 354\,{\rm MeV}$, $f_{\rm D} \gtrsim 64\%$)
PSR J0740+6620	Viable	Viable	Viable	Viable
PSR J0030+0451	Viable	Viable	Viable	Viable
PSR J0437-4715	Viable	Viable	Viable	Viable
HESS J1731-347	–	–	Viable (DM-core SS)	Viable
PSR J5014-4002E	–	–	Viable (DM-halo SS)	Viable (pure SS, $M_{\rm max} = 2.22\,M_\odot$)

We note that interpretations across models depend sensitively on the assumed BDM fraction $f_{\rm D}$, the boson mass m_χ, and which observational constraints are prioritized. For example, Karkevandi *et al.*[28] require that both the $2M_\odot$ mass constraint and the GW170817 tidal deformability bound $\Lambda_{1.4} \lesssim 580$[54] be satisfied with the same value of $f_{\rm D}$, leading them to reject models with $f_{\rm D} \gtrsim 5\%$. However, as we argue, different compact objects may naturally have different values of $f_{\rm D}$, depending on their formation history. Similarly, Liu *et al.*[30] find that high-$f_{\rm D}$ NS configurations are disfavored for $m_\chi \gtrsim 200\,{\rm MeV}$, but this does not rule out high-$f_{\rm D}$ SSs. In our work, the high mass of PSR J5014-4002E[55] is naturally accommodated by a pure SS model with $M_{\rm max} = 2.22\,M_\odot$. Here, we want to mention that Liu *et al.*[30] have studied BDM-admixed NSs using the same EOS of BDM as that in this work. From Fig. 7 in Ref. [30], one finds that the mass and radius observations of XTE J1814-338 could also be explained by BDM-admixed NSs, and the parameter of the BDM model could also be constrained.

Note that although the mass and radius measurements of XTE J1814-338 could also be consistent with BDM-admixed NSs (BDM-NS), BDM-admixed SS interpretation offers a more robust explanation for the extremely small radius inferred for XTE J1814-338. SS matter is self-bound and naturally supports radii in the 6–8 km range even at low masses, whereas obtaining such radii within BDM-NS models typically requires fine-tuning of both the hadronic EOS and the DM fraction. In our framework, the SS interpretation reproduces the observed compactness of XTE J1814-338 with fewer modeling assumptions.

Achieving DM mass fractions as high as $f_{\rm D} \sim 70\%$ cannot be explained by standard accretion from the Galactic halo, which contributes at most $\sim 10^{-5}\,M_\odot$ over a stellar lifetime.[11,39] More plausible scenarios involve the early formation of compact, self-gravitating DM cores—such as from primordial overdensities or DM-rich collapse in regions of enhanced DM density (e.g., subhalo remnants or DM spikes near black holes). These configurations could later accrete baryons and evolve into SSs with high $f_{\rm D}$. Similar ideas have been explored in the context of dark stars[56,57] and two-fluid DM-admixed NSs.[58] Self-interactions, as modeled via the coupling λ, may further promote core formation by suppressing free-streaming and enhancing clumping. Although a full cosmological model is beyond the scope of this work, high-$f_{\rm D}$ configurations remain plausible and warrant further exploration.

We stress that such high values of $f_{\rm D}$ only appear under special circumstances mentioned above and they are **not** expected for ordinary stars since standard halo accretion contributes at most $\sim 10^{-5}\,M_\odot$ over a stellar lifetime. Therefore, our model does **not** affect current understanding of stellar structure and evolution, nor does it conflict with current cosmological models. Also our model does **not** imply that most pulsars contain substantial DM fractions. As shown in Fig. 1, only the remarkably small radius of XTE J1814-338 appears to be exceptional, all other well-measured compact stars (PSR J0740+6620, PSR J0030+0451, PSR J0437-4715, HESS J1731-347) may be explained with $f_{\rm D} \lesssim 30\%$, and in many cases $f_{\rm D} = 0$.

Beyond mass–radius fits and tidal deformability bounds, future observations could distinguish BDM-admixed SSs through spectral and dynamical signatures. NICER and ATHENA are sensitive to redshift, surface gravity, and light bending—all of which are enhanced by the steep potentials of high-$f_{\rm D}$ stars. In the gravitational wave sector, post-merger remnants of NS–SS or SS–SS mergers may exhibit delayed collapse, altered f-mode spectra, or broader emission due to the extended DM halo. These features fall within the detection thresholds of LIGO A+, Einstein Telescope, and Cosmic Explorer. Thus, BDM-admixed compact stars offer not only a compelling explanation for compact objects like XTE J1814-338, but also falsifiable predictions for multimessenger astronomy.

Finally, we note that our two-fluid formalism assumes only gravitational coupling between the SQM and BDM sectors. Future work should investigate the effects of weak or self-annihilating interactions, which could impact stability, cooling, and structure.

In summary, XTE J1814-338 provides a rare observational window into the structure of DM-admixed compact stars. We demonstrate that a high-$f_{\rm D}$ BDM-admixed SS model not only matches the measured mass and radius, but also constrains the BDM particle mass to $m_\chi \lesssim 307(\lambda/\pi)^{1/4}\,{\rm MeV}$. This offers a testable prediction for future high-precision radius measurements and gravitational wave observations.

Acknowledgements. This work was supported by the National Key R&D Program of China (Grant No. 2021YFA0718500). The authors thank professor Renxin Xu for discussions on the mass measurement of XTE J1814-338.

References

[1] Itoh N 1970 *Prog. Theor. Phys.* **44** 291
[2] Bodmer A R 1971 *Phys. Rev. D* **4** 1601

[3] Witten E 1984 *Phys. Rev. D* **30** 272
[4] Farhi E and Jaffe R L 1984 *Phys. Rev. D* **30** 2379
[5] Alcock C, Farhi E, and Olinto A 1986 *Astrophys. J.* **310** 261
[6] Madsen J 1999 *Lect. Notes Phys.* **516** 162
[7] Weber F 2005 *Prog. Part. Nucl. Phys.* **54** 193
[8] Zhang X L, Huang Y F, and Zou Z C 2024 *Front. Astron. Space Sci.* **11** 1409463
[9] Geng J, Li B, and Huang Y 2021 *Innovation* **2** 100152
[10] Qiao G J, Shang L H, Xu R X, Lee K J, Xue Y Q, Zhi Q J, Lu J G, and Bai J T 2025 *JUSTC* **55** 0401
[11] Bramante J and Raj N 2024 *Phys. Rep.* **1052** 1
[12] Grippa F, Lambiase G, and Poddar T K 2025 *Universe* **11** 74
[13] Kini Y, Salmi T, Vinciguerra S, Watts A L, Bilous A, Galloway D K, van der Wateren E, Khalsa G P, Bogdanov S, Buchner J, and Suleimanov V 2024 *Mon. Not. Roy. Astron. Soc.* **535** 1507
[14] Laskos-Patkos P and Moustakidis C C 2025 *Phys. Rev. D* **111** 063058
[15] Zhou T and Huang C 2025 arXiv:2504.08662 [astro-ph.HE]
[16] Zhang C, Pretel J M Z, and Xu R 2025 arXiv:2507.01371 [astro-ph.HE]
[17] Pitz S L and Schaffner-Bielich J 2025 *Phys. Rev. D* **111** 043050
[18] Lopes L L and Issifu A 2025 *Phys. Dark Universe* **48** 101922
[19] Yang S H, Pi C M, and Weber F 2025 *Phys. Rev. D* **111** 043037
[20] Lopes L L 2025 *Astrophys. Space Sci.* **370** 79
[21] Khlopov M Y, Malomed B A, and Zeldovich Y B 1985 *Mon. Not. R. Astron. Soc.* **215** 575
[22] Colpi M, Shapiro S, and Wasserman I 1986 *Phys. Rev. Lett.* **57** 2485
[23] Liu H M, Chu P C, Liu H, Li X H, and Li Z H 2025 arXiv:2501.04382 [nucl-th]
[24] Haensel P, Zdunik J L, and Schaefer R 1986 *Astron. Astrophys.* **160** 121
[25] Navas S, Amsler C, Gutsche T *et al.* 2024 *Phys. Rev. D* **110** 030001
[26] Pi C M, Yang S H, and Zheng X P 2015 *Res. Astron. Astrophys.* **15** 871
[27] Yang S H, Pi C M, Zheng X P, and Weber F 2020 *Astrophys. J.* **902** 32
[28] Karkevandi D R, Shakeri S, Sagun V, and Ivanytskyi O 2022 *Phys. Rev. D* **105** 023001
[29] Shakeri S and Karkevandi D R 2024 *Phys. Rev. D* **109** 043029
[30] Liu H M, Wei J B, Li Z H, Burgio G F, and Schulze H J 2023 *Phys. Dark Univ.* **42** 101338
[31] Eby J, Kouvaris C, Nielsen N G, and Wijewardhana L C R 2016 *J. High Energ. Phys.* **2016** 28
[32] Markevitch M, Gonzalez A H, Clowe D, Vikhlinin A, Forman W, Jones C, Murray S, and Tucker W 2004 *Astrophys. J.* **606** 819
[33] Kaplinghat M, Tulin S, and Yu H B 2016 *Phys. Rev. Lett.* **116** 041302
[34] Sagunski L, Gad-Nasr S, Colquhoun B, Robertson A, and Tulin S 2021 *J. Cosmol. Astropart. Phys.* **01** 024
[35] Pons J A, Reddy S, Prakash M, Lattimer J M, and Miralles J A 1999 *Astrophys. J.* **513** 780
[36] Benvenuto O G and Lugones G 1995 *Phys. Rev. D* **51** 1989
[37] Kettner C, Weber F, Weigel M K, and Glendenning N K 1995 *Phys. Rev. D* **51** 1440
[38] Yasutake N, Maruyama T, and Tatsumi T 2009 *Phys. Rev. D* **80** 123009
[39] Sandin F and Ciarcelluti P 2009 *Astropart. Phys.* **32** 278
[40] Li A, Huang F, and Xu R X 2012 *Astropart. Phys.* **37** 70
[41] Yang S H, Pi C M, and Zheng X P 2021 *Phys. Rev. D* **104** 083016
[42] Yang S, Pi C, Zheng X, and Weber F 2023 *Universe* **9** 202
[43] Yang S H and Pi C M 2024 *J. Cosmol. Astropart. Phys.* **09** 052
[44] Lü W and Wen D 2025 *Phys. Rev. D* **112** 063036
[45] Cromartie H T, Fonseca E, Ransom S M, Demorest P B, Arzoumanian Z, Blumer H, Brook P R, DeCesar M E, Dolch T, Ellis J A, Ferdman R D, Ferrara E C, Garver-Daniels N, Gentile P A, Jones M L, Lam M T, Lorimer D R, Lynch R S, McLaughlin M A, Ng C, Nice D J, Pennucci T T, Spiewak R, Stairs I H, Stovall K, Swiggum J K, and Zhu W W 2020 *Nat. Astron.* **4** 72
[46] Fonseca E, Cromartie H T, Pennucci T T *et al.* 2021 *Astrophys. J. Lett.* **915** L12
[47] Dittmann A J, Miller M C, Lamb F K, Holt I M, Chirenti C, Wolff M T, Bogdanov S, Guillot S, Ho W C G, Morsink S M, Arzoumanian Z, and Gendreau K C 2024 *Astrophys. J.* **974** 295
[48] Salmi T, Choudhury D, Kini Y, Riley T E, Vinciguerra S, Watts A L, Wolff M T, Arzoumanian Z, Bogdanov S, Chakrabarty D, Gendreau K, Guillot S, Ho W C G, Huppenkothen D, Ludlam R M, Morsink S M, and Ray P S 2024 *Astrophys. J.* **974** 294
[49] Vinciguerra S, Salmi T, Watts A L, Choudhury D, Riley T E, Ray P S, Bogdanov S, Kini Y, Guillot S, Chakrabarty D, Ho W C G, Huppenkothen D, Morsink S M, Wadiasingh Z, and Wolff M T 2024 *Astrophys. J.* **961** 62
[50] Choudhury D, Salmi T, Vinciguerra S, Riley T E, Kini Y, Watts A L, Dorsman B, Bogdanov S, Guillot S, Ray P S, Reardon D J, Remillard R A, Bilous A V, Huppenkothen D, Lattimer J M, Rutherford N, Arzoumanian Z, Gendreau K C, Morsink S M, and Ho W C G 2024 *Astrophys. J. Lett.* **971** L20
[51] Doroshenko V, Suleimanov V, Pühlhofer G, and Santangelo A 2022 *Nat. Astron.* **6** 1444
[52] Shawqi S and Morsink S M 2024 *Astrophys. J.* **975** 123
[53] Prix R 2004 *Phys. Rev. D* **69** 043001
[54] Abbott B P, Abbott R, Abbott T D *et al.* 2018 *Phys. Rev. Lett.* **121** 161101
[55] Barr E D, Dutta A, Freire P C C, Cadelano M, Gautam T, Kramer M, Pallanca C, Ransom S M, Ridolfi A, Stappers B W, Tauris T M, Krishnan V V, Wex N, Bailes M, Behrend J, Buchner S, Burgay M, Chen W, Champion D J, Chen C H R, Corongiu A, Geyer M, Men Y P, Padmanabh P V, and Possenti A 2024 *Science* **383** 275
[56] Spolyar D, Freese K, and Gondolo P 2008 *Phys. Rev. Lett.* **100** 051101
[57] Ilie C, Paulin J, and Freese K 2023 *Proc. Nat. Acad. Sci.* **120** e2305762120
[58] Kumar A and Sotani H 2024 *Phys. Rev. D* **110** 063001